

## Research Article

### Optimal Control for Single-Phase Brushless DC Motor with Hall Sensor

<sup>1</sup>Dawei Meng, <sup>2</sup>Xifeng Wang, <sup>1</sup>Yongming Xu and <sup>1</sup>Yufeng Lu

<sup>1</sup>Harbin University of Science and Technology, Harbin, 150080, China

<sup>2</sup>Heilongjiang Institute of Technology, Harbin, 150050, China

**Abstract:** This study deals with the optimization control of a single-phase brushless DC motor (BLDCM) with Hall sensor. A simple modeling method with feasible parameter identification is adopted to meet characteristics of single-phase BLDCM. With the linear Hall sensor feedback, the advantages of current-mode control scheme and soft-commutation scheme are proposed to achieve maximum efficiency over the entire speed range. This thesis also develops a low-cost and high efficiency control for single-phase BLDCM. The hardware test platform has been constructed on a single-chip Field Programmable Gate Array (FPGA) of Cyclone II Family of Altera to verify the performance and feasibility of the proposed optimization control strategies. When using the control scheme with Hall sensor, experimental results show that there are at least a 10% improvement for average value of dc-link current, a 10% improvement for RMS value of phase current and a 40% improvement for peak value of phase current.

**Keywords:** BLDCM, FPGA, hall sensor, optimization control method

## INTRODUCTION

Along with the rapid development of economy, it is essential for the electronic products to be elaborated and sophisticated and the internal functions are various and high speed. The phase windings of BLDCM can be classified as single-phase or 3-phase, their flux distribution can be either sinusoidal or trapezoidal. Single-phase BLDCM is less expensive and easier to manufacture compared to 3-phase BLDCM and is widely used in low-cost and low-power applications. However, it exhibits zero torque points at certain rotor positions. Even though these dead points could be avoided by applying an asymmetric air gap, this deteriorates motor characteristics in torque and efficiency.

Because of rapid development of integrated circuit, the integration of control and drive ICs have been widely implemented in BLDCM. The linear Hall sensor provides the information of rotor position and velocity via signal processing technique. However, there are some unsuitable for high temperature environment. Sun *et al.* (2007) analyze the drive of single-phase brushless dc motors based on torque. Rubaai *et al.* (2002) have a research of the development and implementation of an adaptive fuzzy-neural-network controller for brushless drives. Son *et al.* (2008) study the integrated MOSFET inverter module of low-power drive system. Xia *et al.* (2009) have a study of the control strategy for four-switch 3 phase brushless dc motor using single current sensor. Su and Mckeever (2004) analyze the low-cost

sensor less control of brushless dc motors with improved speed range. Pan and Fang (2008) study a phase-locked-loop-assisted internal model adjustable-speed controller for BLDC motors. Sathyan *et al.* (2009) have a research of the FPGA-based novel digital PWM control scheme for BLDC motor. Liu *et al.* (2007) analyze the commutation torque ripple minimization in direct-torque-controlled pm brushless dc drives.

With the development of digital integrated circuit, digital motor control systems have been widely implemented with software and hardware based on microcontrollers or FPGA. These approaches provide flexibility and are suitable for motor drive applications. For simple structure and requirement of single-phase BLDCM motor, it's easy to employ to slim type application of consumer electronics.

Moreover, due to the characteristics of wide speed range, small size, easy controllability and long lifetime expectancy, single-phase BLDC motors are now the major choice for forced air cooling in PC, NB and other information appliances. The proposed control schemes have been implemented on a single-chip FPGA controller to verify the performance and feasibility for single-phase BLDCM. Experimental verification has been carried out on a single-phase BLDCM control system.

## STRUCTURE AND MATHEMATICAL MODELING

Figure 1 shows an initially designed single-phase BLDCM. It is an outer rotor type and consists of 4 poles



Fig. 1: The overall diagram of our method

and four slots. To solve the optimum problem, effective design variables capable of significantly influencing the objective function need to be chosen.

The marked feature of single-phase BLDCM is the asymmetric air gap to eliminate dead point. If dead point, where the developed torque value is zero, exists in single phase BLDCM, there is a possibility that the motor will stop at the dead-point and be unable to start. The stator winding can be modeled as a winding resistance in series with a winding inductance and a back-EMF voltage. The voltage equation describing the dynamic behavior of single-phase BLDCM is given as follow:

$$v = L_s \frac{di}{dt} + iR_s + v_{emf} \tag{1}$$

where,

$v$  : The phase voltage

$i$  : Phase current

$R_s$  : The winding resistance

$L_s$  : The winding inductance

$v_{emf}$  : The back-EMF voltage induced by rotor flux variation and the value is proportional to motor speed and can be computed by:

$$v_{emf} = K_E \cdot \omega_r \tag{2}$$

where,

$\omega_r$  : The rotor velocity

$K_E$  : The back-EMF constant which is associated with the form of nonlinear flux distribution in this application

For the mechanical system, the developed torque must overcome the inertial acceleration torque, friction torque and the load torque. Therefore, the torque-speed characteristics can be formulated as:

$$T_e = J_m \frac{d\omega_r}{dt} + B_m \omega_r + T_L \tag{3}$$

where, the inertial acceleration torque is represented by the product of the moment of inertia  $J_m$  and the angular acceleration  $d\omega_r/dt$ . The load torque referred to the motor shaft, while the friction torque is the product of the rotor velocity and viscous friction coefficient  $B_m$ .

According to previous equations, the modeling of single-phase BLDCM can be represented by a block diagram as shown in Fig. 2:

### MODEL VERIFICATION

According to previous description, a simple modeling method with an illustrated parameter identification scheme for single-phase BLDCM has been proposed. Using the open-loop voltage-mode of hard-commutation scheme (Fig. 3) shows the consistency of the proposed model and the real motor, it can be seen that simulation results are close to experiment measurements under different duty ratio. Figure 4 shows the RMS value of phase current and rotor speed curves under different duty ratio, the simulation result is also close to experiment

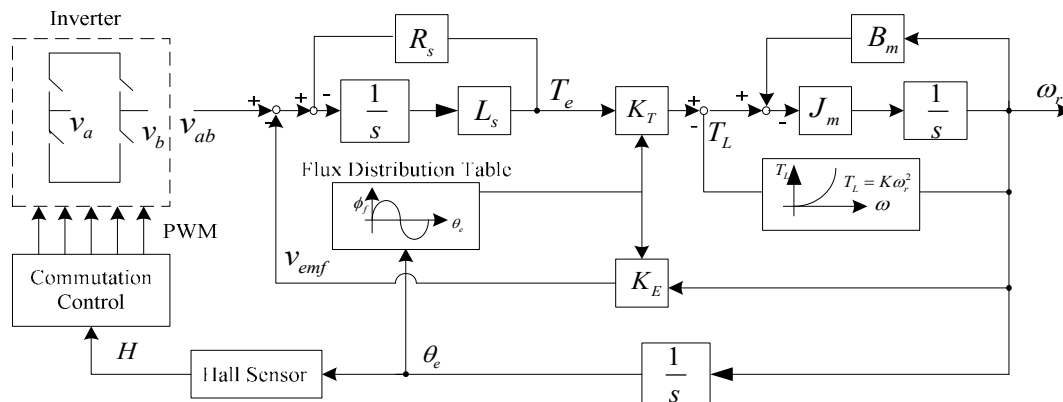
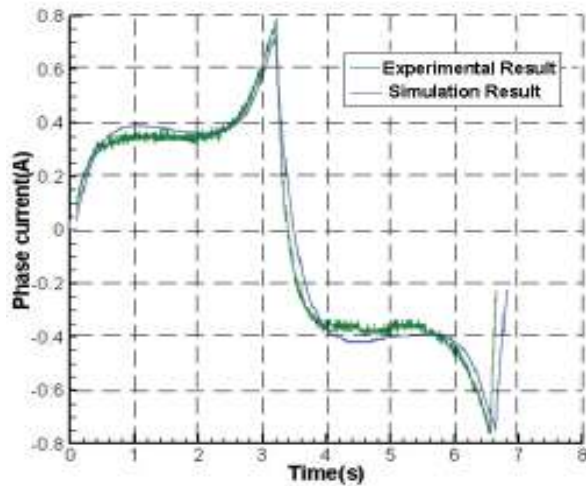
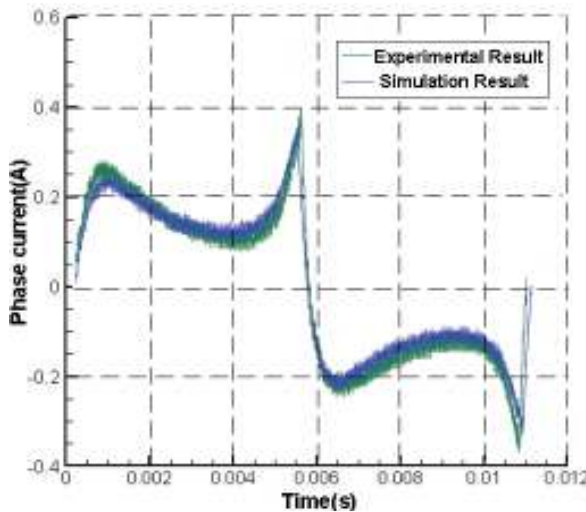


Fig. 2: Block diagram for modeling of the single-phase BLDCM



(a)



(b)

Fig. 3: Phase current comparison between simulation result and experiment measurement (a) duty = 100%, (b) duty = 50%

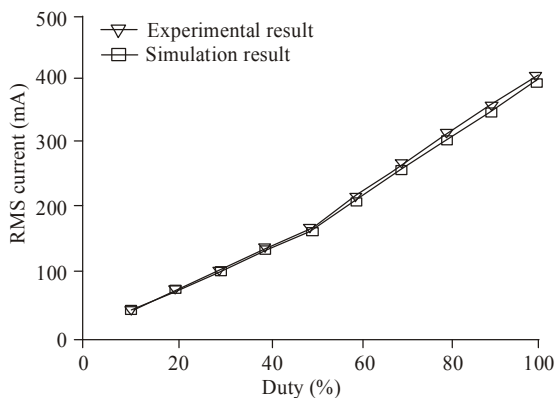


Fig. 4: The RMS value of phase current and rotor speed curve

measurement. That is, above of all confirm the validity of the proposed model.

### EFFICIENCY OPTIMATIZATION CONTROL SCHEME

Both of hard-commutation and soft-commutation scheme are still sensitive to the rotor flux distribution, so the overall efficiency will be seriously degraded in wide speed control applications. This research develops the efficiency optimization control scheme based on closed-loop current-mode control scheme for single-phase BLDCM.

Moreover, the advantage of soft-commutation control at high speed operation will be adopted to widen the speed control range and to reduce the current spike. This research uses the digital PI controller to realize the current-regulation which ensures that the measured stator current tracks the required values accurately and to shorten the transient interval as much as possible. Figure 5 shows the continuous time equivalent of current-loop control system, where the controller block is represented by typical PI regulator structure.

The controller design is typically based on specifications concerning the required closed loop bandwidth and phase margin. In our application, we suppose that the system bandwidth  $f_{CL}$  equals to about one tenth of the switching frequency and at least a 45 degree phase margin PM. So, parameters  $K_P$  and  $K_I$  have to determine to guarantee these requirements.

### HARDWARE TEST PLATFORM AND EXPERIMENTAL RESULT ANALYSIS

The microelectronics technologies have become a major trend. The digital control scheme has the advantages of simple circuitry, software control and flexibility in various applications. In order to verify the validity of the developed control strategies with linear Hall sensor, a FPGA-based control system is setup for the experiments. Two fast periodic interrupts with 20 kHz performs the A/D converter synchronization, PWM generation, sensor algorithm, start-up control and current-loop control. It should be noted that both the control algorithm with, are realized in this ISR. The synchronous sampling technique is adopted to sense the phase current.

The FPGA controller performs the real-time control algorithms, including the PI algorithm, start-up control and closed-loop current-mode control. Experiments on the developed control strategies with Hall sensor are carried out. Using the single-phase BLDCM drive setup described in the previous section, the system

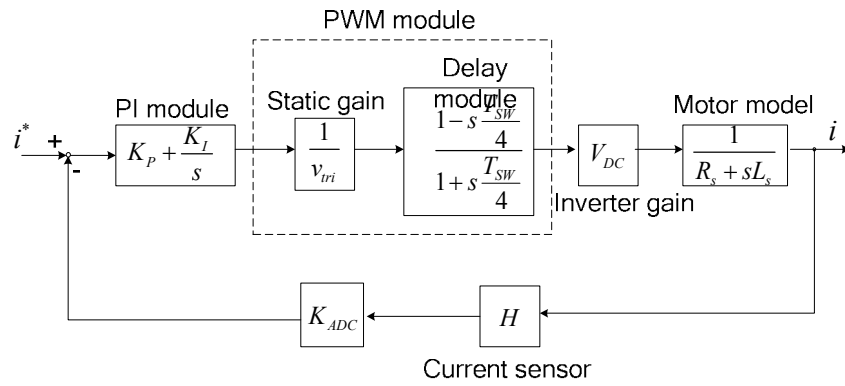


Fig. 5: The continuous time equivalent of current-loop control system

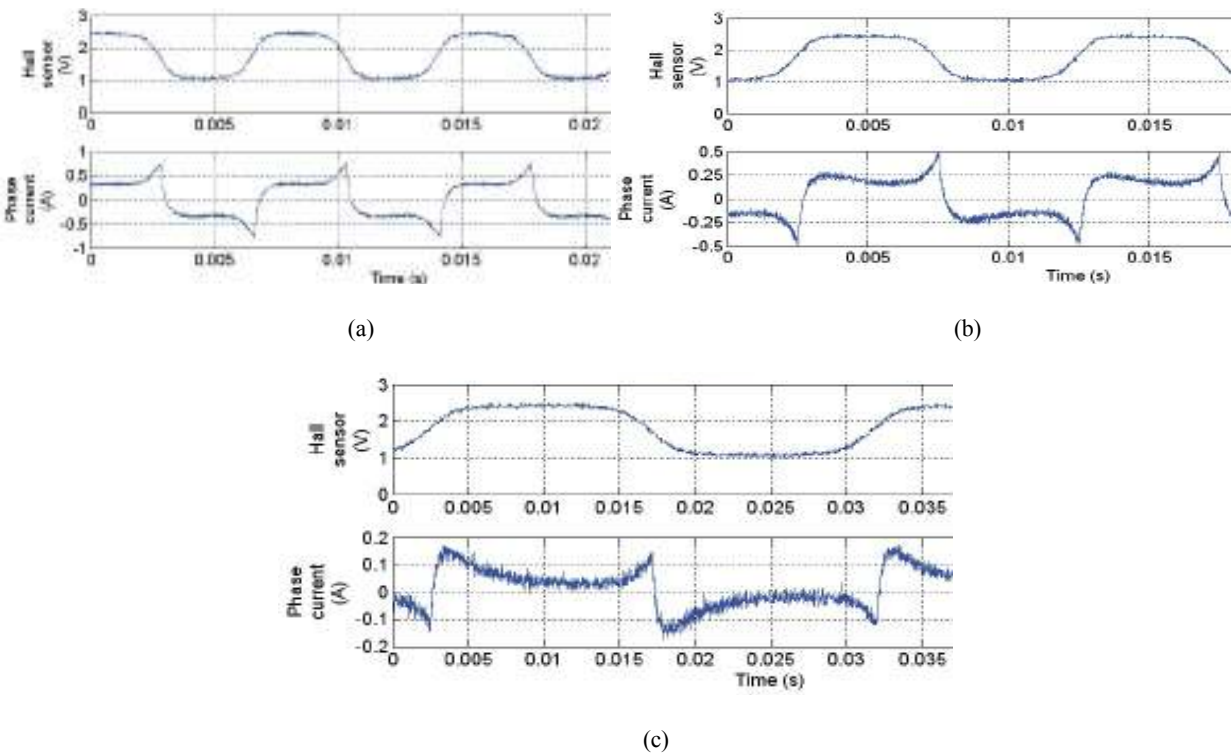


Fig. 6: Steady-state response when using the open-loop voltage-mode control of hard commutation scheme (a) 4000 RPM, (b) 3000 RPM, (c) 1000 RPM

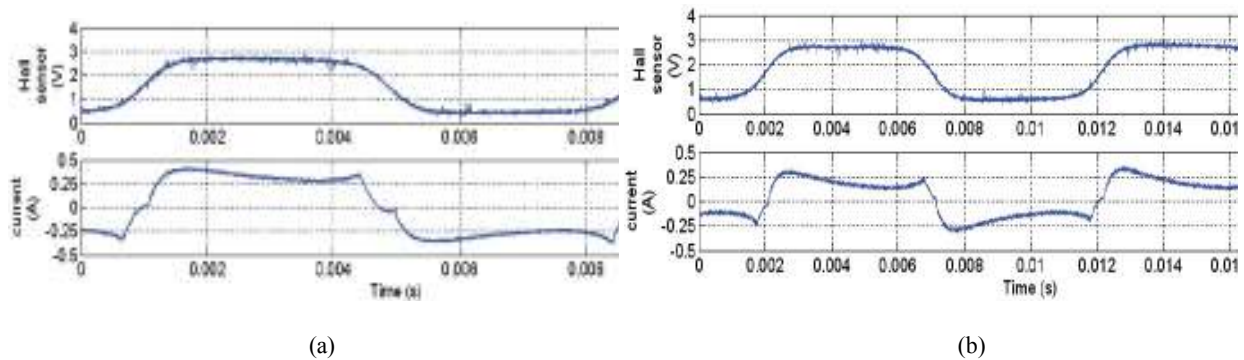


Fig. 7: Steady-state response when using the soft-commutation scheme (a) 4000 RPM, (b) 3000 RPM

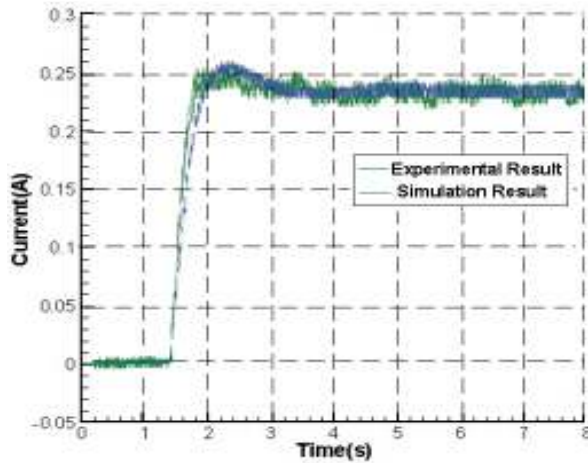


Fig. 8: The step response of current-loop control system at zero current by 400 mA step input

performance are evaluated for various steady-state and transient operating conditions.

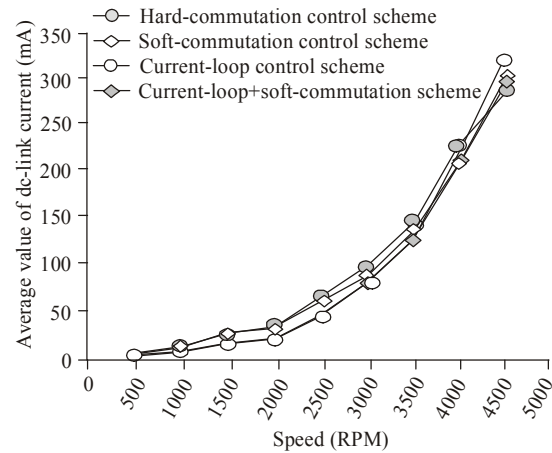
The steady-state response when using the open-loop voltage-mode control of hard-commutation scheme at 4000, 3000 and 1000 RPM, respectively. The waveform can be seen in Fig. 6.

Figure 7 shows the steady state response when using the open-loop voltage-mode control of soft-commutation scheme at 4000, 3000 and 1000 RPM, respectively. In Fig. 7(a), the phase voltage waveform exists a blanking time of 15% commutation cycle. Besides, from phase current waveform, there are a 40% reduction of peak value and a 10% reduction of RMS value. However, In Fig. 7(b), the blanking time is shorten to 5% commutation cycle and the improvements of peak current is only 5% and RMS current is only 2%. As expected, the soft-commutation control is only suitable for high speed operation.

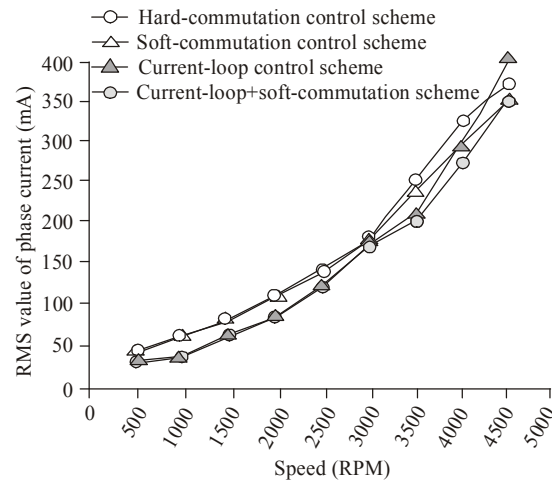
The efficiency optimization control scheme is the combination of closed-loop current-mode control for low and middle speed operation and open-loop voltage-mode control of soft-commutation scheme for high speed operation. Figure 8 shows the step response of current-loop control system at zero current by 400 mA step input.

Using the single-phase BLDCM drive setup described in the previous section, the system performance are evaluated for various steady-state and transient operating conditions.

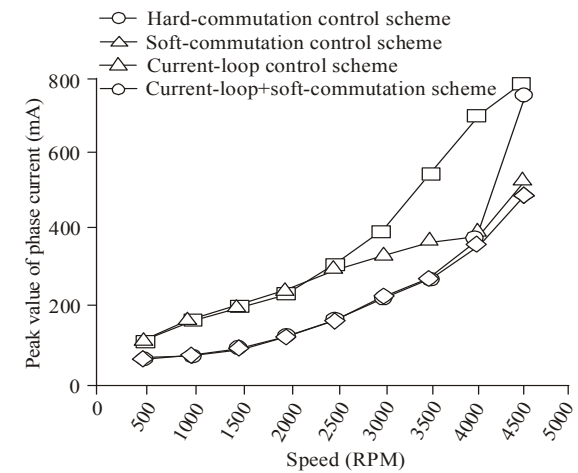
In order to verify the proposed control strategy, the overall efficiency is compared by various control schemes. Figure 9(a) shows the average value of dc-link current versus rotor speed. For entire speed range, the curve of hard- commutation control scheme has higher value than other control methods, which means that it needs more input power to drive the fan motor at the same speed. Figure 9(b) shows the RMS value of phase current versus rotor speed. Similarly, the developed control scheme has relatively lower value for four methods, which means that it has higher utility ratio of



(a) Average value of dc-link current versus rotor speed



(b) RMS value of phase current versus rotor speed



(c) Peak value of phase current versus rotor speed

Fig. 9: Statistics curves of various control schemes

current and so as to electrical output power for fan motor. Figure 9(c) shows the peak value of phase

current versus rotor speed. Obviously, the peak value has significant reduction for entire speed range and this will reduce the acoustic noise and power circuit rating.

### CONCLUSION

This study presents the efficiency optimization control for single-phase BLDCM with Hall sensor. The control scheme has been verified by computer simulation based on the proposed model. Besides, the drive system is implemented by FPGA and some experimental results have been shown to verify the performance and feasibility.

This study presents an efficiency optimization control scheme for single-phase BLDCM with linear Hall sensor. To produce the maximum output power, the each back-EMF control system with Hall sensor on a digital signal processing hardware platform. The FPGA controller performs the real-time control algorithms, start-up control and current-loop control, etc. Then, the practical realization issues and analyses of experimental results are also presented.

In summary, this study presents efficiency optimization control for single-phase BLDCM with Hall sensor. The developed control strategies are first verified by proposed model and then fulfill on a real single-phase BLDCM with Hall sensor based on FPGA controller.

### REFERENCES

- Liu, Y., Z.Q. Zhu and D. Howe, 2007. Commutation torque ripple minimization in direct-torque-controlled PM brushless DC drives. *IEEE T. Ind. Electron*, 43(4): 1012-1021.
- Pan, C.T. and E. Fang, 2008. A phase-locked-loop-assisted internal model adjustable-speed controller for BLDC motors. *IEEE T. Ind. Electron*, 55(9): 3415-3425.
- Rubaii, A., D. Ricketts and M.D. Kankam, 2002. Development and implementation of an adaptive fuzzy-neural-network controller for brushless drives. *IEEE T. Ind. Appl.*, 38(2): 441-447.
- Sathyan, A., N. Milivojevic, Y.J. Lee, M. Krishnamurthy and A. Emadi, 2009. An FPGA-based novel digital PWM control scheme for BLDC motor. *IEEE T. Ind. Electron*, 56(8): 3040-3049.
- Son, Y.C., K.Y. Jang and B.S. Suh, 2008. Integrated MOSFET inverter module of low-power drive system. *IEEE T. Ind.*, 44(3): 878-886.
- Su, G.J. and J.W. Mckeever, 2004. Low-cost sensorless control of brushless DC motors with improved speed range. *IEEE T. Power Electr.*, 19(2): 296-302.
- Sun, L., Q. Fang and J. Shang, 2007. Drive of single-phase brushless DC motors based on torque. *IEEE T. Magn.*, 43(1): 46-50.
- Xia, C., Z. Li and T. Shi, 2009. A control strategy for four-switch 3 phase brushless DC motor using single current sensor. *IEEE T. Ind. Electron*, 56(6): 2058-2066.